

## Measurement of three-dimensional flame structure by combined laser diagnostics<sup>†</sup>

Takashi Ueda, Masayasu Shimura, Mamoru Tanahashi\* and Toshio Miyauchi

*Department of Mechanical and Aerospace Engineering, Tokyo Institute of Technology,  
2-12-1 Ookayama, Meguro-ku, Tokyo, 152-8550 Japan*

(Manuscript Received March 21, 2009; Revised April 16, 2009; Accepted April 20, 2009)

---

### Abstract

To investigate three-dimensional flame structures of turbulent premixed flame experimentally, dual-plane planar laser induced fluorescence (PLIF) of CH radical has been developed. This dual-plane CH PLIF system consists of two independent conventional CH PLIF measurement systems and laser beam from each laser system are led to parallel optical pass using the difference of polarization, and CH PLIF is conducted in two parallel two-dimensional cross sections. The newly-developed dual-plane CH PLIF is combined with single-plane OH PLIF and stereoscopic particle image velocimetry (PIV) to clarify the relation between flame geometry and turbulence characteristics. The laser sheets for single-plane OH PLIF and stereoscopic PIV measurement are located at the center of two planes for CH PLIF. The separation between these two planes is selected to 500  $\mu\text{m}$ . The measurement was conducted in relatively high Reynolds number methane-air turbulent jet premixed flame. The experimental results show that various three-dimensional flame structures such as the handgrip structure, which has been shown by three-dimensional direct numerical simulations (DNS), are included in high Reynolds number turbulent premixed flame. It was shown that the simultaneous measurement containing newly-developed dual-plane CH PLIF is useful for investigating the three-dimensional flame structures. To analyze the flame structures quantitatively, the flame curvature was estimated by using the CH and OH PLIF images, and the probability density function (pdf) of the curvatures was compared with the results of DNS. It was revealed that the minimum radius of curvature of the flame front coincides with Kolmogorov length. However, the feature of pdf of the flame curvature is slightly different from result of DNS, if the curvature was estimated from experimental results in two-dimensional cross section. On the other hand, the feature of pdf of mean curvature that calculated from triple-plane PLIF results is similar to that obtained from three-dimensional DNS.

*Keywords:* Flame structures; PIV; PLIF; Turbulent premixed flame

---

### 1. Introduction

In the recent three-dimensional direct numerical simulations (DNS) [1-6], characteristics of the turbulent premixed flames have been investigated extensively, and local flame structures which are hardly expected from theoretical classifications such as the turbulent combustion diagram [7] have been reported.

Three-dimensional flame structures, which are caused by strong fine scale eddies in turbulence, appear even in laminar flamelet regime in the turbulent combustion diagram. The importance of these structures should be investigated by experiment.

To investigate turbulent flame structures experimentally, planar laser-induced fluorescence (PLIF) [8, 9] of molecules and radicals produced in chemical reactions, such as OH [10], CO [11], CH [12-14] and CH<sub>2</sub>O [15], are commonly used. Since OH radicals show high concentration in the burned gas, OH PLIF measurement is useful to separate the unburned mixture and the burned gas. Although the edges of OH

---

<sup>†</sup> This paper was presented at the 7th JSME-KSME Thermal and Fluids Engineering Conference, Sapporo, Japan, October 2008.

\*Corresponding author. Tel.: +82 32 872 309681 3 5734 3181, Fax.: +82 32 868 171681 3 5734 3181

E-mail address: kykim@inha.ac.krmtanahas@mes.titech.ac.jp

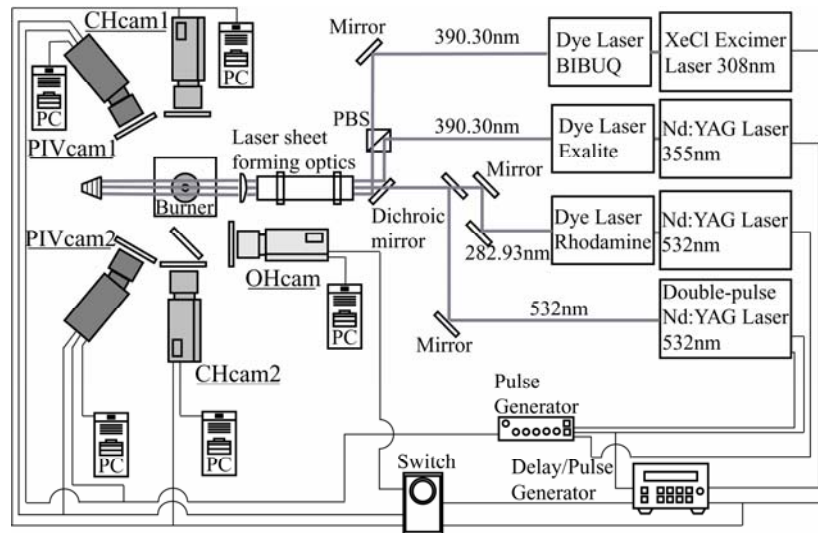


Fig. 1. Schematic diagram of the simultaneous dual-plane CH PLIF, single-plane OH PLIF and stereoscopic PIV measurement.

radical distribution may correspond to the flame fronts for low Reynolds number turbulent flames, there is a possibility that the flame fronts do not exist at the edge of OH radicals in high Reynolds number cases in which flame front is significantly distorted and multiply folded. On the other hand, CH PLIF measurement has been used to investigate characteristics of the flame fronts in turbulence because CH radicals are produced at the flame front and have very narrow width enough to represent the reaction zones. However, only from the CH PLIF measurement, it is hard to distinguish the unburned gases from burned gases. To overcome these defects in single radical PLIF, simultaneous OH and CH PLIF measurement has been developed and applied for turbulent non-premixed flames [16].

In addition to the PLIF measurement, particle image velocimetry (PIV) has been adopted to measure the turbulence characteristics near the flame [17, 18]. Recently, simultaneous CH, OH and velocity measurement has been reported [19, 20] for investigate the flame structures. Furthermore, to investigate the dynamics of turbulent premixed flame, CH double-pulsed PLIF measurement [21] and simultaneous CH double pulsed PLIF/OH PLIF and stereoscopic PIV measurement [22] and simultaneous stereo PIV and double-pulsed acetone PLIF [23] were developed. However, almost all studies were restricted to measurement in two-dimensional cross section. Although reconstruction of the three-dimensional flame structure has been reported [24], it is difficult to investi-

gate the instantaneous three-dimensional flame structures.

In this study, to investigate three-dimensional flame structures of turbulent premixed flame, dual-plane PLIF of CH radicals has been developed. The newly-developed dual-plane CH PLIF is combined with single-plane OH PLIF and stereoscopic PIV, which can investigate the three velocity components, to investigate the relation between flame geometry and turbulence characteristics.

## 2. Experimental method

### 2.1 Dual-plane CH PLIF measurement system

The schematic diagram of the experimental setup for simultaneous measurement is shown in Fig. 1. By combining two independent CH PLIF systems, the dual-plane CH PLIF system is comprised. For CH PLIF measurement, the  $Q_1(7,5)$  transition of the  $B^2\Sigma-X^2\Pi(0,0)$  band at 390.30 nm is excited and fluorescence from the  $A-X(1,1)$ ,  $(0,0)$  and  $B-X(0,1)$  bands between 420 and 440 nm is detected. CH radical is excited by two laser systems. First dye laser (Lambda Physik, Scanmate2) is pumped by a XeCl excimer laser (Lambda Physik, LPX 110I, 308 nm, 200 mJ/pulse) with BiBuQ dye in *p*-dioxane solvent and second dye laser (Sirah Cobra-stretch) is pumped by a Nd:YAG laser (SpectraPhysics, Quanta Ray PRO-230-10, 355 nm, 400 mJ/pulse) with Exalite389 dye in *p*-dioxane solvent. These laser systems generate laser pulses of about 18-20 and about 20-22 mJ/pulse,

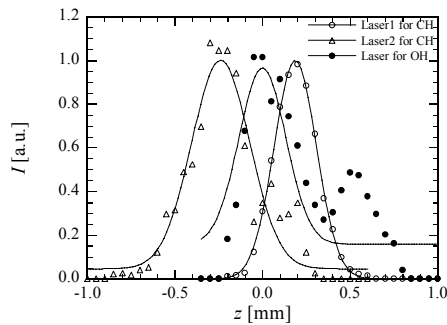


Fig. 2. Profiles of laser sheets for dual-plane CH PLIF and OH PLIF.

respectively. Laser beams from each laser systems have vertical polarization. The polarization of beam from the XeCl excimer with the dye laser changed into horizontal direction by using several mirrors. These beams are lead to a polarizing beam splitter (PBS) and parallel beams are generated. The parallel beams are expanded into laser sheets by laser sheet forming optics.

Fluorescence from excited CH radicals are detected by two intensified CCD cameras (Andor Technology, iStar DH734-25U-03,  $1024 \times 1024$  pixels) fitted with 105 mm/f2.8 lens (Nikon, Micro-Nikkor) and optical filters (SCHOTT, KV418 and BG39). These cameras are located on the opposite side of the burner, and optical axes are set to be perpendicular to the laser sheet. Fig. 2 shows the intensity profiles for the lasers of PLIF measurements. These profiles are measured by traversing a photodiode with a  $10 \mu\text{m}$  pinhole. It is found that the laser beams are shaped into about  $250 \mu\text{m}$  thickness and the separation between the two laser sheets that can be changed by regulating the PBS is set to  $500 \mu\text{m}$ .

### 2.2 Single-plane OH PLIF measurement system

For single-plane OH PLIF measurement, the  $Q_1(7)$  transition of the  $A^2\Sigma-X^2\Pi(1,0)$  band at 282.93 nm is excited and fluorescence from the  $A-X(1,1)$ , (0,0) and  $B-X(0,1)$  bands between 306 and 320 nm is detected. The laser system consists of a Nd:YAG laser (Continuum, Powerlite9030, 532 nm, 200 mJ/pulse) and a dye laser (Lambda physik, Scanmate2) with Rhodamine 590 dye in *p*-dioxane solvent. Laser beam is led to laser sheet forming optics and illuminate the measurement region. The fluorescence from the excited OH radicals were imaged onto the third intensified CCD camera (Princeton Instruments, PI-MAX 51RB-

G1,  $512 \times 512$  pixels) fitted with UV lens (Nikon, UV-Nikkor, 105 mm/f4.5) and optical filters (SCHOTT, WG-305 and UG-11). The laser beam is shaped into about  $300 \mu\text{m}$  thickness, and the laser sheet located at the center of the two laser sheets for CH PLIF as shown in Fig. 2.

### 2.3 Stereoscopic PIV measurement system

Stereoscopic PIV system consists of a double pulsed Nd:YAG laser (New Wave Research, Mini-Lase III, 532 nm, 50 mJ/pulse), an optical system and two CCD cameras (Princeton Instruments, MegaPlus II ES4020,  $2048 \times 2048$  pixel) with 200 mm/f4 lens (Nikon, Micro-Nikkor). CCD cameras are located at each side of the intensified CCD cameras for CH PLIF with about 20 degree. To focus on all over the measurement region clearly, the Scheimpflug condition [25] is applied. The double-pulsed laser sheets which are located at the center of the two laser sheets for CH PLIF illuminate the measuring region and scattered light by tracer particles is recorded by the CCD cameras.  $\text{Al}_2\text{O}_3$  with  $0.18 \mu\text{m}$  diameter are used for tracer particles.

### 2.4 Experimental apparatus

Fig. 3(a) shows a turbulent jet burner used in this study. This burner has a main jet nozzle and a surrounding nozzle for flame holding. The inner diameter of the main and the surrounding nozzles are 10 mm and 70 mm, respectively. Fig. 3(b) shows CH chemiluminescence images and OH PLIF images. Note that these images are combined images obtained at different measurement positions ( $x/D = 5, 10, 15$ ). Table 1 shows experimental conditions and turbulence characteristics of inert flow at center of the jet nozzle. Here,  $x$  is distance from the jet exit,  $Re_D$  is Reynolds number based on the nozzle diameter ( $D$ ) and mean axial velocity at the jet exit,  $Re_\lambda$  is Reynolds number based on Taylor microscale  $\lambda$  and r.m.s. of velocity fluctuation ( $u'_{rms}$ ),  $u_m$  is mean velocity,  $l$  is integral length scale and  $\eta$  is Kolmogorov length.  $S_L$  ( $= 0.399$  m/s) is laminar burning velocity and  $\delta_f$  ( $= 41.2 \mu\text{m}$ ) is laminar flame thickness which is defined based on kinematic viscosity and  $S_L$  [7]. The characteristics were measured by a hotwire constant temperature anemometer with x-probe (Kanomax Japan, Model0250R, tungsten,  $\Phi 5 \mu\text{m}$ ) in preliminary experiments. These conditions are classified into the corrugated flamelets in the turbulent combustion diagram by Peters [7]. In this study,

Table 1. Experimental conditions.

$U_0$ [m/s]	$x/D$	$Re_D$	$Re_\lambda$	$u_m$ [m/s]	$u'_{rms}$ [m/s]	$l$ [mm]	$\lambda$ [mm]	$\eta$ [ $\mu$ m]	$l/\delta_f$	$u'_{rms}/S_L$
10	5	6667	93.4	11.40	1.15	6.21	0.998	58.0	150.8	2.88

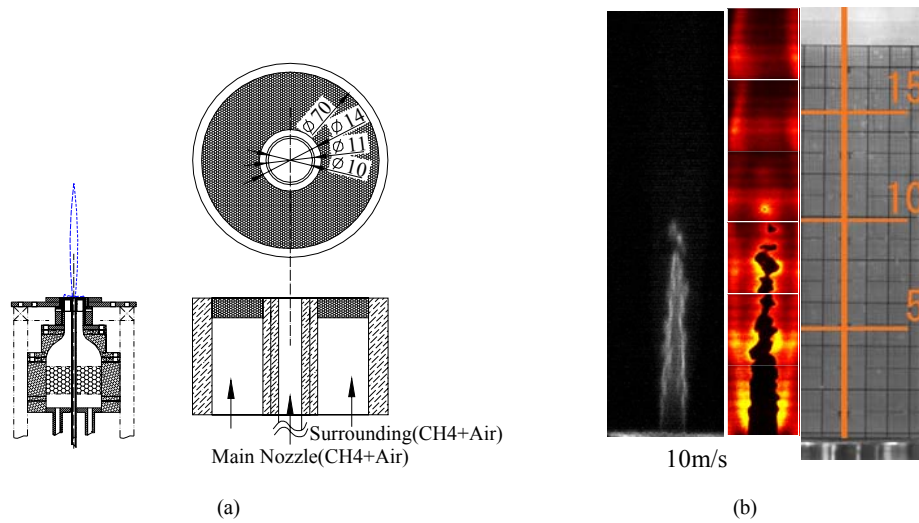


Fig. 3. Schematic of a turbulent jet burner (a) and a CH chemiluminescence image and OH fluorescence image of turbulent jet pre-mixed flame (b).

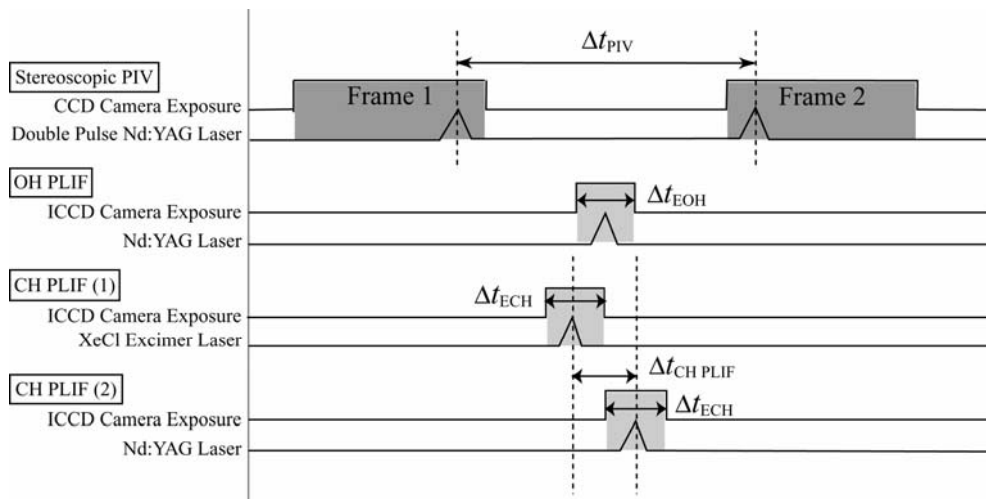


Fig. 4. Timing diagram of the simultaneous dual-plane CH PLIF, single-plane OH PLIF and stereoscopic PIV measurements.

simultaneous measurement of dual-plane CH PLIF, single-plane OH PLIF and stereoscopic PIV is conducted for  $U_0 = 10$  m/s. Equivalence ratio  $\phi$  is fixed to 1.0 for the main flame and 0.86 for the surrounding flame. PLIF and PIV were conducted at axial distance of  $x/D = 5$ , where the turbulence is fully developed.

From turbulence and flame characteristics, the pixel resolutions are set to 28.8  $\mu$ m/pixel for CH PLIF, 57.5  $\mu$ m/pixel for OH PLIF and 8.8  $\mu$ m/pixel for stereoscopic PIV and the measurement regions are 29.5 mm  $\times$  29.5 mm for CH and OH PLIF, 18 mm  $\times$  18 mm for stereoscopic PIV.

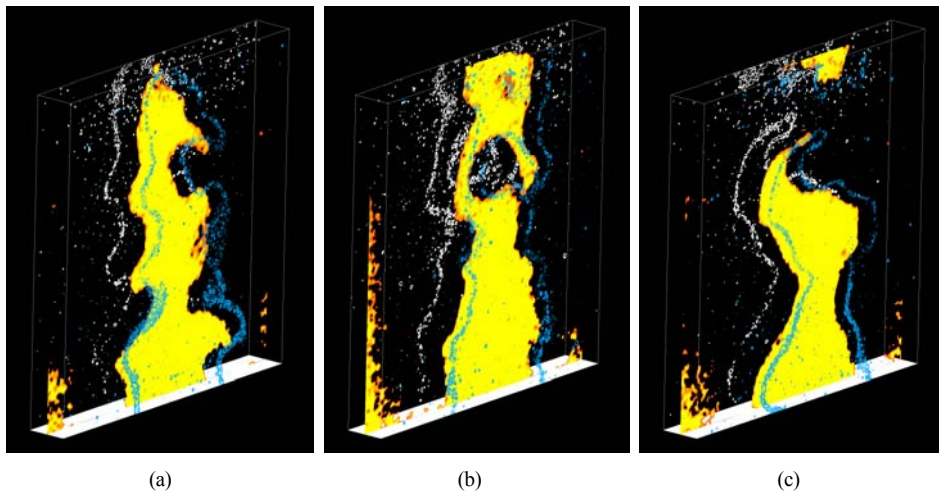


Fig. 5. Typical three-dimensional flame structure. (a), (b) and (c) represent different realization.

### 2.5 Timing control for simultaneous dual-plane CH PLIF, single-plane OH PLIF and stereoscopic PIV measurements

Fig. 4 shows the timing diagram of the simultaneous dual-plane CH PLIF, single-plane OH PLIF and stereoscopic PIV measurements. In this study, to take CH images on each plane by different camera, CH PLIF on two planes was conducted with short time difference of 50 ns. This time difference is short enough for the turbulent flame to maintain its structure. After the first CH PLIF, OH PLIF was conducted with 25 ns delay. These PLIF measurements were conducted between the first and second frame for stereoscopic PIV. From the turbulence characteristics in measurement region, time interval of PIV ( $\Delta t_{PIV}$ ) is set to 4.1  $\mu$ s. For rejecting flame radiation, exposure time for PIV is set to about 250  $\mu$ s by controlling liquid-crystal shutters. To optimize signal-to-noise ratio, gate time of image intensifiers for dual-plane CH PLIF and single-plane OH PLIF are set to 30 ns [20]. Timing control of this system is conducted by two pulse generators (Stanford Research Systems, DG535 and LabSmith, LC880) and delay generators inside of intensified CCD cameras.

### 3. Experimental results

Fig. 5 shows typical three-dimensional flame structures of turbulent premixed flame obtained by the simultaneous dual-plane CH PLIF, single-plane OH PLIF and stereoscopic PIV measurements. In this

figure, the isolines drawn by blue and white represent fluorescence intensity distributions of CH radicals in each plane, and the yellow area represents the unburned mixture obtained by fluorescence intensity distribution of OH radicals. The visualized distance between two measured planes is twenty times the real scale for easy understanding. This simultaneous measurement can investigate flame structures from a three-dimensional perspective as shown in Fig. 5(a). Fig. 5(b) shows that engulfment of burned gas near the centerline of the jet and the burned gas forms complicated three-dimensional structure. Fig. 5(c) shows that flame is split and an isolated pocket of unburned mixture is generated. Fig. 6 shows more complex flame structure. From the distribution of CH radicals in the rear plane, flame front is connected to the main flame (indicated by white arrows). On the other hand, the pocket of unburned mixture is generated in the center plane (white circle) and annular flame front is produced in the front plane (yellow circle). This structure may represent the handgrip structure, which has been suggested by DNS [6]. The present results show that the simultaneous dual-plane CH PLIF, single-plane OH PLIF and stereoscopic PIV measurement is useful for investigation of the three-dimensional flame structures. In this study, to analyze flame structure quantitatively, the flame front curvature is estimated from the present experimental results and is compared with previous three-dimensional DNS. The curvature of the flame front is defined by

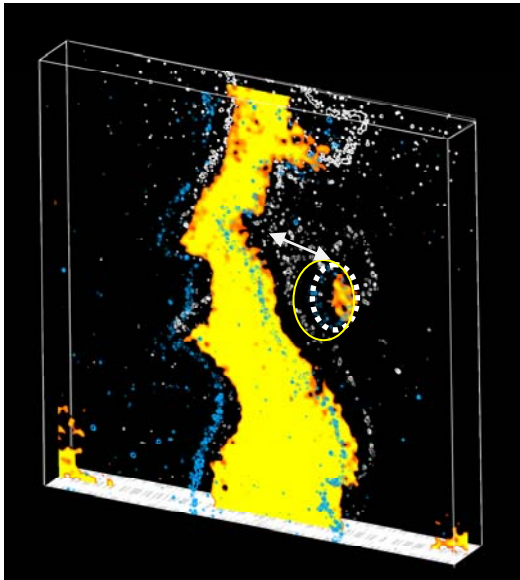


Fig. 6. An example of handgrip structure.

$$k = \nabla \cdot \mathbf{n}, \quad (1)$$

where  $\mathbf{n}$  denotes normal vector with respect to the flame front. If the principal curvatures can be estimated as  $k_1$  and  $k_2$ ,  $k$  is represented by

$$k = (k_1 + k_2) / 2. \quad (2)$$

In the analysis of three-dimensional DNS, the principal curvature of three-dimensional flame surface can be estimated. However, from the experimental results, it is quite hard to estimate those. Therefore, in the present study, the curvature is evaluated by the following procedure.

- (1) The flame front is identified on the three parallel planes from CH and OH PLIF images.
- (2) On the center plane (OH PLIF plane), the curvature of the flame front ( $k_{c1}$ ) is estimated from Eq. 1.
- (3) A plane perpendicular to the center plane including the flame front position on the center plane is defined.
- (4) Intersection point of the above-mentioned plane and flame front on the CH PLIF planes are identified.
- (5) From the flame front position on the OH PLIF plane and two flame front positions on the CH PLIF planes, the flame curvature ( $k_{c2}$ ) is estimated by finding a circle that have the three flame front points on the circumference.
- (6) The mean curvature is calculated by  $k_e = (k_{c1} + k_{c2}) / 2$ .

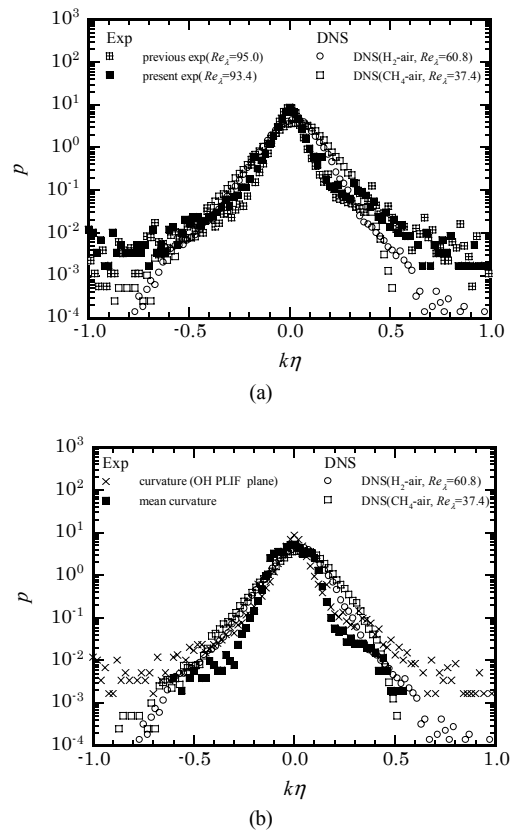


Fig. 7. Probability density functions of the curvature of the flame front (a), probability density functions of the mean curvature (b).

In Fig. 7(a), probability density functions (pdf) of the flame curvature obtained in OH PLIF plane ( $k_{c1}$ ) are compared with the results obtained by previous study of simultaneous CH OH PLIF and stereoscopic PIV measurements for turbulent premixed flames at swirl burner [26] and three-dimensional DNS [27]. Equivalence ratio is 1.0 both for the experiment and DNS. Note that the curvature of the flame front for DNS represents mean value of principal curvatures of three-dimensional surface. The curvature is non-dimensionalized by the Kolmogorov length ( $\eta$ ). Two experimental results coincide with each other. The maximum values of  $|k\eta|$  are about 1.0 both for the experiment and DNS. Therefore, the minimum radius of curvature is the Kolmogorov length. However, the shapes of the pdf obtained by the experiments are slightly different from those by DNS. This will be caused by the curvature estimation only from two-dimensional cross section in the experiments. It should be noted that curvature of the flame front has been reported by many previous studies [3, 23], whe-

reas all studies reported those in dimensional form or non-dimensionalized by laminar flame properties. In Fig. 7(b), the mean curvature ( $k_e$ ) is compared with that from DNS. For comparison, pdf of  $k_{cl}$  is also presented. Probability for small curvature decreases for  $k_e$  compared with  $k_{cl}$ . This feature is similar to that obtained from DNS. However, the separation of PLIF planes determines the largest curvature and should be reduced to improve the results.

#### 4. Summary

In this study, simultaneous dual-plane CH PLIF, single-plane OH PLIF and stereoscopic PIV measurement was developed. It was demonstrated that three-dimensional flame structures can be investigated by this newly-developed simultaneous measurement in methane-air turbulent premixed jet burner. This simultaneous measurement revealed that the minimum radius of curvature of the flame front coincides with Kolmogorov length. The feature of pdf of mean curvature obtained by the present measurement is similar to that obtained from DNS.

#### Acknowledgment

This work is partially supported by Grant-in-Aid for Scientific Research (S) (No.18106004) of Japan Society for the Promotion of Science.

#### References

- [1] M. Tanahashi, M. Fujimura and T. Miyauchi, Coherent fine-scale eddies in turbulent premixed flames, *Proc. Combust. Inst.*, 28 (2000) 529-535.
- [2] M. Tanahashi, Y. Nada, Y. Ito and T. Miyauchi, Local flame structure in the well-stirred reactor regime, *Proc. Combust. Inst.*, 29 (2002) 2041-2049.
- [3] K. W. Jenkins and R. S. Cant, Curvature effects on flames kernels in a turbulent environment, *Proc. Combust. Inst.*, 29 (2002) 2023-2029.
- [4] S. Sreedhara and K. N. Lakshmisha, Autoignition in a non-premixed medium: DNS studies on the effects of three-dimensional turbulence, *Proc. Combust. Inst.*, 29 (2002) 2051-2059.
- [5] J. B. Bell, M. S. Day and J. F. Grcar, Numerical simulation of premixed turbulent methane combustion, *Proc. Combust. Inst.*, 29 (2002) 1987-1993.
- [6] Y. Nada, M. Tanahashi and T. Miyauchi, Effect of turbulence characteristics on local flame structure of H<sub>2</sub>-air premixed flames, *J. Turbulence*, 5 (2004) 16.
- [7] N. Peters, *Turbulent combustion*. London: Cambridge Press (2000).
- [8] R. K. Hanson, Combustion diagnostics: planar imaging techniques. *Proc. Combust. Inst.*, 21 (1986) 1677-1691.
- [9] M. J. Dyer and D. R. Crosley, Fluorescence imaging for flame chemistry. *Proc. Int. Conf. Laser*, 84 (1985) 211-218.
- [10] M. D. Smooke, Y. Xu, R. M. Zurn, P. Lin, J. H. Frank and M. B. Long, Computational and experimental study of OH and CH radicals in axisymmetric laminar diffusion flames. *Proc. Combust. Inst.*, 24 (1992) 813-821.
- [11] J. M. Seitzman, J. Haumann and R. K. Hanson, Quantitative twophoton LIF imaging of carbon monoxide in combustion gases. *Appl. Opt.*, 26 (1987) 2892-2899.
- [12] M. G. Allen, R. D. Howe and R. K. Hanson, Digital imaging of reaction zones in hydrocarbon-air flames us in planar laser-induced fluorescence of CH and C<sub>2</sub>. *Opt. Lett.*, 11 (1986) 126-128.
- [13] C. D. Carter, J. M. Donbar and J. F. Driscoll, Simultaneous CH planar laser-induced fluorescence and particle imaging velocimetry in turbulent non-premixed flames. *Appl. Phys.*, 66 (1998) 129-132.
- [14] M. S. Mansour, N. Peters and Y. C. Chen, Investigation of scalar mixing in the thin reaction zones regime using a simultaneous CH-LIF/Rayleigh laser technique. *Proc. Combust. Inst.*, 27 (1998) 767-773.
- [15] S. Bockle, J. Kazenwadel, T. Kunzelmann, D.-I. Shin, C. Schulz and J. Wolfrum, Simultaneous single-shot laser-based imaging of formaldehyde, OH, and temperature in turbulent flames. *Proc. Combust. Inst.*, 28 (2000) 279-286.
- [16] J. M. Donbar, J. F. Driscoll and C. D. Carter, Reaction zone structure in turbulent nonpremixed Jet flames from CH-OH PLIF imaging, *Combust. Flame*, 122 (2000) 1-19.
- [17] P. A. M. Kalt, J. H. Frank and R. W. Bilger, Laser imaging of conditional velocities in premixed propane/air flames by simultaneous OH PLIF and PIV, *Proc. Combust. Inst.*, 27 (1998) 751-758.
- [18] J. O. Sinibaldi, J. F. Driscoll, C. J. Mueller, J. M. Donbar and C. D. Carter, Propagation speeds and stretch rates measured along wrinkled flames to assess the theory of flame stretch, *Combust. Flame*, 133 (2003) 323-334.
- [19] P. S. Kothnur, M. S. Tsurikov, N. T. Clemens, J. M. Donbar and C. D. Carter, Planar imaging of CH,

- OH and velocity in turbulent non-premixed jet flames, *Proc. Combust. Inst.*, 29 (2002) 1921-1927.
- [20] M. Tanahashi, S. Murakami, G.-M. Choi, Y. Fukuchi and T. Miyauchi, Simultaneous CH-OH PLIF and stereoscopic PIV measurements of turbulent premixed flames, *Proc. Combust. Inst.*, 30 (2005) 1665-1672.
- [21] M. Tanahashi, S. Taka, M. Shimura and T. Miyauchi, CH double-pulsed PLIF measurement in turbulent premixed flame, *Exp. Fluids*, 45 (2008) 323-332.
- [22] M. Tanahashi, S. Taka, T. Hirayama, Y. Minamoto and T. Miyauchi, Local burning velocity measurements in turbulent jet premixed flame by simultaneous CH DPPLIF/OH PLIF and stereoscopic PIV, *Proc. of 14th Int. Symp. Appl. Laser Tech. Fluid Mech.*, (2008).
- [23] S. A. Filatyev, M. P. Thariyan, R. P. Lucht and J. P. Gore, Simultaneous stereo particle image velocimetry and double-pulsed planar laser-induced fluorescence of turbulent premixed flames, *Combust. Flame*, 150 (2007) 201-209.
- [24] M. Tanahashi, S. Inoue, M. Shimura, S. Taka, G.-M. Choi and T. Miyauchi, Reconstructed 3D flame structures in noise-controlled swirl-stabilized combustor, *Exp. Fluids*, 45(3) (2008) 447-460.
- [25] A. K. Prasad, Scheimpflug stereocamera for particle image velocimetry in liquid flows, *Appl. Opt.*, 34(30) (1995) 7092-7099.
- [26] S. Inoue, S. Taka, S. Kato, Y. Nada, M. Tanahashi and T. Miyauchi, Measurements of local flame structures of turbulent premixed flames by simultaneous CH-OH PLIF and stereoscopic PIV, *Proc. 5th ASPACC*. (2005) 385-388.
- [27] S. Kikuta, M. Tanahashi and T. Miyauchi, Three-dimensional direct numerical simulation for CH<sub>4</sub>-air turbulent premixed flames, *Proc. 42nd Jpn. Symp. Combust.* (2004) 355-356.



**Takashi Ueda** received his B.S. degree in Mechano-Aerospace Engineering from Tokyo Institute of Technology, Japan, in 2008. Mr. Ueda is currently in Master course at Department of Mechanical and Aerospace Engineering, Tokyo Institute of Technology, Tokyo, Japan. Mr. Ueda's research interests include turbulent combustion.



**Masayasu Shimura** received his B.S. degree in Mechano-Aerospace Engineering from Tokyo Institute of Technology, Japan, in 2005. He then received his M.S. from Tokyo Institute of Technology in 2006. Mr. Shimura is currently in Ph.D candidate at Department of Mechanical and Aerospace Engineering, Tokyo Institute of Technology, Tokyo, Japan. Mr. Shimura's research interests include noise control of turbulent combustion.



**Mamoru Tanahashi** received his B.S. degree in Mechanical Engineering, Science from Tokyo Institute of Technology, Japan, in 1990. He then received his M.S. and Dr. Eng. from Tokyo Institute of Technology in 1992 and 1996, respectively. Prof. Tanahashi is currently an Associate Professor of Department of Mechanical and Aerospace Engineering, Tokyo Institute of Technology, Tokyo, Japan. Prof. Tanahashi's research interests include turbulence and combustion.



**Toshio Miyauchi** received his B.S. degree in Mechanical Engineering from Tokyo Institute of Technology, Japan, in 1971. He then received his M.S. and Ph.D. degrees from Tokyo Institute of Technology in 1973 and 1981, respectively. Prof. Miyauchi is currently a Professor of Department of Mechanical and Aerospace Engineering, Tokyo Institute of Technology, Tokyo, Japan. Prof. Miyauchi's research interests include turbulence and combustion.